

Geometrizing Quantum Dynamics of a Bose-Einstein Condensate

Changyuan Lyu^{1,*}, Chenwei Lv^{1,*} and Qi Zhou^{1,2,†}

¹*Department of Physics and Astronomy, Purdue University, West Lafayette, Indiana 47907, USA*

²*Purdue Quantum Science and Engineering Institute, Purdue University, West Lafayette, Indiana 47907, USA*

 (Received 17 June 2020; accepted 12 November 2020; published 15 December 2020)

We show that quantum dynamics of Bose-Einstein condensates in the weakly interacting regime can be geometrized by a Poincaré disk. Each point on such a disk represents a thermofield double state, the overlap between which equals the metric of this hyperbolic space. This approach leads to a unique geometric interpretation of stable and unstable modes as closed and open trajectories on the Poincaré disk, respectively. The resonant modes that follow geodesics naturally equate fundamental quantities including the time, the length, and the temperature. Our work suggests a new geometric framework to coherently control quantum systems and reverse their dynamics using SU(1,1) echoes. In the presence of perturbations breaking the SU(1,1) symmetry, SU(1,1) echoes deliver a new means to measure these perturbations such as the interactions between excited particles.

DOI: 10.1103/PhysRevLett.125.253401

Geometries may arise as emergent phenomena in certain quantum systems. Prototypical examples include the AdS/CFT correspondence [1,2], the ER = EPR conjecture [3–6], and scale invariant tensor networks [7–10]. In these examples, a prerequisite for the emergent hyperbolic geometries is the existence of strong correlations in quantum many-body systems. A question thus arises as to whether one could use weakly interacting systems, where gauge theory/gravity duality is unavailable at the moment, to reveal some intriguing geometries.

In this work, we show that quantum dynamics of weakly interacting bosons have deep roots in the hyperbolic geometry. Whereas such dynamics has been extensively studied [11–16], our geometric approach has a number of unique advantages compared to the previous works. On the theoretical side, it leads to new understandings of prior experimental results. It shows that a fundamental concept of dynamical instability has an underlying geometric interpretation, corresponding to open trajectories on a Poincaré disk, a prototypical model for the hyperbolic surface. In sharp contrast, stable modes are mapped to closed trajectories, and the transition from stable to unstable mode can be visualized by the change of topology of the trajectories on the Poincaré disk.

In practice, our approach provides experimentalists with a powerful tool to access and manipulate new quantum dynamical phenomena. It delivers SU(1,1) echoes to reverse any initial state of any excitation mode once interactions of BECs change, as analogous to spin echoes overcoming the dephasing in spin systems [17,18]. Moreover, it could be used as a new framework to detect perturbations that breaks the SU(1,1) symmetry, in the same spirit of using spin echoes to extract a wide range of useful information when spins are interacting with each other [19–23]. Finally, our

scheme based on the $su(1,1)$ algebra and its underlying geometric representation applies to any systems with the SU(1,1) symmetry, similar to spin echoes broadly applied to systems whose constituents obey the $su(2)$ algebra. Our scheme thus can be used to reverse quantum dynamics in a wide range of systems and explore information scrambling via out-of-time ordering correlators (OTOC) [24–27].

To be specific, this geometric approach correlates the time in quantum dynamics to the length in the hyperbolic space, and to the temperature that captures thermalization of a subsystem, as follows:

$$\tilde{L} = |\xi|t, \quad (1)$$

$$\tilde{T} = -\frac{1}{2} \ln^{-1} \tanh(2\tilde{L}), \quad (2)$$

where \tilde{L} is the dimensionless length in a hyperbolic geometry and \tilde{T} is the dimensionless temperature. $|\xi|$ is an energy scale characterizing the Hamiltonian and t is the time. Each point on the Poincaré disk is assigned a unique SU(1,1) coherent state, and the overlap between two nearby SU(1,1) coherent states, which is denoted by $F_{z,z+dz}$, is equated to the metric of a Poincaré disk,

$$ds^2 = 4(1 - F_{z,z+dz}) = \frac{4(dx^2 + dy^2)}{(1 - x^2 - y^2)^2}, \quad (3)$$

where (x, y) denote Cartesian coordinates.

We consider a Hamiltonian

$$H = \sum_{\vec{k}} E_{\vec{k}} c_{\vec{k}}^\dagger c_{\vec{k}} + \frac{\tilde{U}}{2V} \sum_{\vec{k}, \vec{k}', \vec{q}} c_{\vec{k}+\vec{q}}^\dagger c_{\vec{k}'-\vec{q}}^\dagger c_{\vec{k}'} c_{\vec{k}}, \quad (4)$$

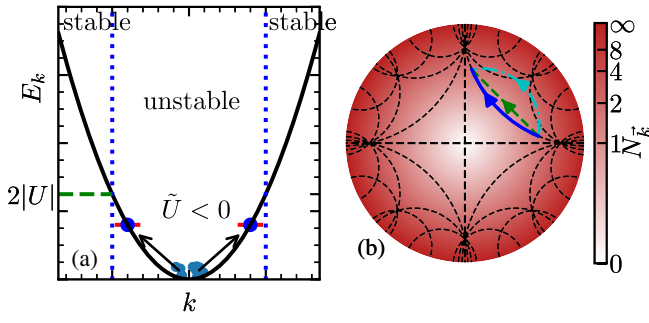


FIG. 1. (a) A negative interaction scatters bosons from the condensate to states with opposite momenta. States with small kinetic energies have exponentially growing occupations. (b) Each point on a Poincaré disk represents a TFD. The color scale highlights the particle number or equivalently, the effective temperature. Dashed straight lines and curves represent the geodesics. Arrowed curves denote trajectories representing dynamical evolutions of the quantum system. The blue curve following the geodesic corresponds to an extreme of the time spent in a quench dynamics.

where $\tilde{U} = 4\pi\hbar^2 a_s/M$, $c_{\vec{k}}^\dagger$ ($c_{\vec{k}}$) is the creation (annihilation) operator for bosons with the momentum \vec{k} . Starting from $t = 0$, $a_s(t)$ is tuned dynamically from either zero or a small value using the magnetic or optical Feshbach resonance [28], as shown in Fig. 1. Our results based on the $su(1,1)$ algebra apply to both quenching a_s or an arbitrary $a_s(t)$ [29].

Though a BEC with attractive interactions is not stable [11,15,16], coherent dynamics is achievable within a timescale before significant losses of particles occur [40]. We first focus on short-time dynamics in which the particle number at a finite momentum, $N_{\vec{k} \neq 0}$, is small such that interactions among excitations are negligible. The quantum dynamics is governed by a Hamiltonian, $H_{\text{eff}} = \sum_{\vec{k}} H_{\vec{k}}$,

$$H_{\vec{k}}(t) = \xi_0(\vec{k})K_0 + \xi_1(\vec{k})K_1 + \xi_2(\vec{k})K_2, \quad (5)$$

where $K_0 = \frac{1}{2}(c_{\vec{k}}^\dagger c_{\vec{k}} + c_{-\vec{k}} c_{-\vec{k}}^\dagger)$, $K_1 = \frac{1}{2}(c_{\vec{k}}^\dagger c_{-\vec{k}} + c_{\vec{k}} c_{-\vec{k}}^\dagger)$ and $K_2 = (1/2i)(c_{\vec{k}}^\dagger c_{-\vec{k}}^\dagger - c_{\vec{k}} c_{-\vec{k}})$, $\xi_0(\vec{k}) = 2(E_{\vec{k}} + \tilde{U}|\Psi_0|^2)$, $\xi_1(\vec{k}) = 2\text{Re}U$, $\xi_2(\vec{k}) = -2\text{Im}U$, $U = \tilde{U}\Psi_0^2$, and $\Psi_0 = \sqrt{N_0/V}e^{i\theta}$ is the condensate wave function. $\vec{\xi} = \{\xi_0, \xi_1, \xi_2\}$ is an external field, analogous to the magnetic field in the case of $SU(2)$, and its strength, $\xi = \sqrt{\xi_0^2 - \xi_1^2 - \xi_2^2}$, characterizes the energy scale. For instance, when $\xi_0^2 > \xi_1^2 + \xi_2^2$, the energy spectrum is given by $(m + 1/2)\xi$, where m is an integer. The above equations show that the dynamics at different \vec{k} are decoupled. This model can be realized using a wide range of apparatuses [29].

The Hamiltonian in Eq. (5) with arbitrary choices of parameters, $\xi_{1,2,3}$, can be generated by three operators, K_0 , K_1 , and K_2 , which satisfy

$$\begin{aligned} [K_1, K_2] &= -iK_0, & [K_0, K_1] &= iK_2, \\ [K_2, K_0] &= iK_1. \end{aligned} \quad (6)$$

Any propagator,

$$P(t) = \text{T}e^{-i \int_0^t dt' H_{\vec{k}}(t')}, \quad (7)$$

is an element in $SU(1,1)$ [41], where T is the time-ordering operator. Such $SU(1,1)$ symmetry was recently revisited and a special type of echo applicable to an initial state of the vacuum in periodically driven bosons was discussed [42,43]. Since the global $U(1)$ phase does not affect physical observables, we consider the quotient, $SU(1,1)/U(1)$, whose element is created by two operations,

$$R(\varphi_0) = e^{-i\varphi_0 K_0}, \quad B(\varphi_1, 0) = e^{-i\varphi_1 K_1}, \quad (8)$$

which correspond to a rotation and a boost, respectively. A generic boost along an arbitrary direction is given by $B(\varphi_1, \varphi_2) = e^{-i(\varphi_1 K_1 + \varphi_2 K_2)}$.

Equation (8) provides us with a parametrization of the propagators using a Poincaré disk [41,44], as shown in Fig. 1(b). A similar approach was revisited very recently to consider geometric phases in the adiabatic limit [45]. Whereas both the $SU(1,1)$ symmetry of the Hamiltonian and the geometric representation of $SU(1,1)/U(1)$ are known in the literature [41,44], many fundamental questions remain unexplored. For instance, whether the metric of the Poincaré disk defined geometrically has any correspondence to physical quantities of the quantum system? Does a geodesic, the shortest distance between two points, leads to any significant observations in quantum dynamics? We will answer these questions in the following discussions.

To establish a one-to-one correspondence between the quantum dynamics and a Poincaré disk, we consider the vacuum, $|\Psi(0)\rangle = |0\rangle_{\vec{k}}|0\rangle_{-\vec{k}}$, where $c_{\vec{k}}|0\rangle_{\vec{k}} = 0$. The two operators in Eq. (8) deliver a wave function, $|z\rangle = R(\varphi_0)B(\varphi_1, 0)R^\dagger(\varphi_0)|\Psi(0)\rangle$, which is written as

$$|z\rangle = \sqrt{1 - |z|^2} \sum_n z^n |n\rangle_{\vec{k}} |n\rangle_{-\vec{k}}, \quad (9)$$

where $z = -ie^{-i\varphi_0} \tanh \frac{\varphi_1}{2}$ and $|n\rangle_{\vec{k}} = c_{\vec{k}}^{\dagger n} |0\rangle / \sqrt{n!}$. In high energy physics, the expression in Eq. (9) is called a thermofield double state (TFD) state [3–6,24,25]. In quantum optics, it is referred to as a two-mode squeezed state, which can be created through nondegenerate parametric amplification [46]. Creating squeezed states from squeeze operators has been well studied in quantum optics [47], and such a connection with BECs has also been recently studied [43]. Equation (9) can be derived using explicit forms of the boost and rotation operators [29].

Since $|z| = |x + iy| \leq 1$, we identify each TFD in Eq. (9) with a unique point on the Poincaré disk.

Tracing over half of the system in TFD leaves the other half with a thermal density matrix,

$$\rho_{\bar{k}} = \text{Tr}_{-k} |z\rangle\langle z| = \mathcal{Z}^{-1} \sum_n e^{-\frac{nE_{\bar{k}}}{k_B T}} |n\rangle_{\bar{k}} \langle n|_{\bar{k}}, \quad (10)$$

similar to Hawking radiation and Unruh effects [48,49]. In Eq. (10), we have identified the Euclidean distance to the center of the disk $|z|$ with a temperature

$$\tilde{T} \equiv \frac{k_B T}{E_k} = -\frac{1}{2} \ln^{-1} |z|, \quad (11)$$

and $\mathcal{Z} = 1 - e^{-E_{\bar{k}}/k_B T}$. Each point on the Poincaré disk can be assigned with a temperature and the boundary circle corresponds to $T = \infty$. In quantum information, the closeness between two states is often characterized by their overlap, i.e., their fidelity [50]. Here, the fidelity between TFDs, $F_{z,z'} = |\langle z'|z\rangle|^2$, is written as

$$|\langle z'|z\rangle|^2 = \frac{(1 - |z|^2)(1 - |z'|^2)}{|1 - z^* z'|^2}. \quad (12)$$

Consider two TFDs close to each other on the Poincaré disk, i.e., $z' = z + dz$, from the above expression, we obtain Eq. (3). The fidelity between TFDs thus corresponds to the metric of a Poincaré disk. The metric of a Poincaré disk can also be correlated to the complexities of the SU(1,1) coherent states [51].

We now consider quenching $a_s(t)$ from zero to a finite negative value. When $E_{\bar{k}} > 2|U|$ or, equivalently, $\xi^2 > 0$, the growth of $n_{\bar{k}}$ is bounded from above and is referred as to a stable mode. On the Poincaré disk, it is described by a closed loop, as shown in Fig. 2(b). When $E_{\bar{k}} = 2|U|$, ξ vanishes and the topology of the trajectory changes. When $E_{\bar{k}} < 2|U|$, i.e., $\xi^2 < 0$, the well-known dynamical instability occurs and $n_{\bar{k}}$ grows exponentially, mimicking the inflation in the early Universe [14]. On the Poincaré disk, any unstable mode corresponds to an open trajectory, starting from the origin and extending to the circular boundary. However, it takes infinite time to reach there, since the boundary of the Poincaré disk corresponds to infinity.

When $E_k = |U|$, starting from the center of the Poincaré disk, the trajectory follows the diameter, i.e., a geodesic. The Euclidean distance to the center is written as

$$|z(t)| = \begin{cases} \left(1 - \frac{\xi^2}{\xi_1^2 + \xi_2^2} \frac{1}{\sinh^2(\frac{|\xi|t}{2})}\right)^{-\frac{1}{2}}, & \xi^2 < 0, \\ \left(1 + \frac{\xi^2}{\xi_1^2 + \xi_2^2} \frac{1}{\sin^2(\frac{|\xi|t}{2})}\right)^{-\frac{1}{2}}, & \xi^2 > 0. \end{cases} \quad (13)$$

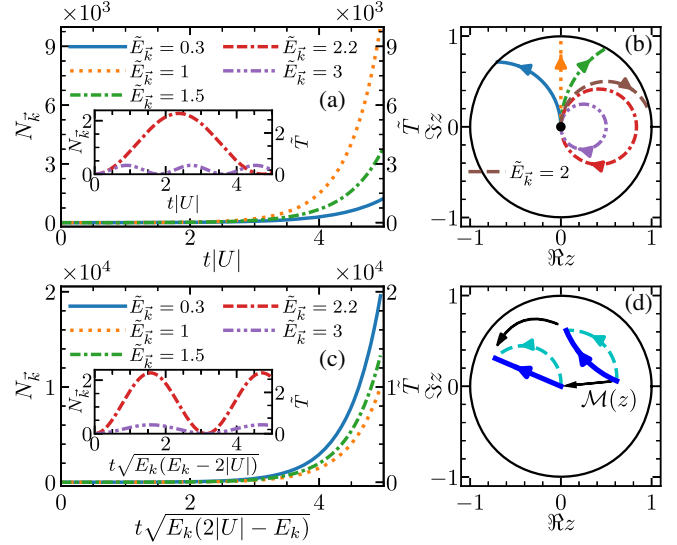


FIG. 2. (a) The dependence of $N_{\bar{k}}$ (left vertical axis) and the rescaled temperature \tilde{T} (right vertical axis) as a function of time. $\tilde{E}_{\bar{k}} = E_{\bar{k}}/|U|$. When U is fixed, the resonant mode has the fastest growth. (b) The stable(unstable) modes are mapped to closed (open) trajectories on the Poincaré disk. The resonant mode moves along the geodesic. (c) When $|\xi|$ is fixed, the resonant mode has the slowest growth. (d) A Möbius transformation maps an arbitrary initial state to the vacuum at the center of the Poincaré disk. The geodesic becomes a straight line and retains its length.

We see from Eq. (13) that, if we fix $\xi_1^2 + \xi_2^2$, $|z(t)|$ grows fastest when $\xi_0 = 0$, i.e., when the system moves along the geodesic. Under this situation

$$|z(t)|_g = \tanh\left(\frac{|\xi|}{2} t\right). \quad (14)$$

Using the metric in Eq. (3), the length along the geodesic is given by

$$\tilde{L} = \int_0^{|\xi|t} \frac{2dx}{1-x^2} = |\xi|t. \quad (15)$$

We thus have proved Eq. (1). Using Eqs. (11), (14), (15), it is also straightforward to prove Eq. (2). It is worth pointing out that, once $|\xi|$ is fixed, Eq. (13) shows that the geodesic corresponds to the slowest growth among unstable modes. As seen from numerical results plotted in Fig. 2(c), the resonant mode does grow slower than other unstable modes. For off-resonant modes, the trajectories are no longer geodesics and the length along such a trajectory as a function of the time has an expression similar to Eq. (15) (Supplemental Material [29]).

If the initial scattering length is finite, the ground state is no longer a vacuum. The quantum dynamics starts from a point away from the center of the Poincaré disk. A Möbius transformation preserving the metric, $z' = \mathcal{M}(z) = (\alpha z + \beta)/(\beta^* z + \alpha^*)$, $|\alpha|^2 - |\beta|^2 = 1$, could

map the origin to any other point on the disk, and thus all phenomena remain the same compared with starting from a vacuum. For any initial and final states, $|z_1\rangle$ and $|z_2\rangle$, the quantum dynamics could follow a geodesic, which in general is not a straight line, using a Hamiltonian,

$$H/|\xi| = \frac{-\text{Im}z_1z_2^*}{|z_1-z_2||z_1z_2^*-1|} (c_k^\dagger c_{-k} + c_{-k} c_k^\dagger) + \frac{i(z_2-z_1+|z_1|^2z_2-|z_2|^2z_1)}{2|z_1-z_2||z_1z_2^*-1|} c_k^\dagger c_{-k}^\dagger + \text{H.c.} \quad (16)$$

To realize the Hamiltonian in Eq. (16), it is required that one could tune θ in Eq. (5) [29].

We now turn to periodic drivings. Consider an example that is directly relevant to current experiments,

$$H_1 = 2(E_{\vec{k}} + U)K_0 + 2UK_1, \quad 0 < t < t_1, \quad (17)$$

$$H_2 = 2E_{\vec{k}}K_0, \quad t_1 < t < T_d, \quad (18)$$

where the period $T_d = t_1 + t_2$. It corresponds to periodically modifying the interaction strength in Eq. (4). When $a_s = 0$, the propagator from $t = t_1$ to $t = T_d$ is given by Eq. (8), i.e., a rotation about the center of the Poincaré disk. Such drivings allow us to manipulate both the stable and unstable modes [29]. A particularly interesting case is a quantum revival of the initial state at the end of the second period. We emphasize that such a revival is accessible for any initial state, and any H_1 in Eq. (17), not requiring a vacuum as the initial state nor a Hamiltonian satisfying the resonant condition [14,42]. We consider an arbitrary $H_1 = w_0K_0 + w_1K_1 + w_2K_2$ with a field strength w . The Baker-Hausdorff-Campbell formula decomposes the propagator $\mathcal{U}_1 = e^{-iH_1t_1}$ into

$$\mathcal{U}_1 = e^{-i\zeta_1 K_0} e^{-i\eta_1 (K_1 \cos \phi_1 + K_2 \sin \phi_1)} e^{-i\zeta_1 K_0}, \quad (19)$$

where $\zeta_1 = \arctan((w_0/w) \tan(wt_1/2))$, $\phi_1 = \arccos(w_1/\sqrt{w_1^2 + w_2^2})$, and $\eta_1 = 2\text{arcsinh}((\sqrt{w_1^2 + w_2^2}/w) \sin(wt_1/2))$.

A quantum revival on a Poincaré disk requires that $(\mathcal{U}_2\mathcal{U}_1)^2 = 1$. Using the identity $B(\eta \cos \phi, \eta \sin \phi) R(\pi) B(\eta \cos \phi, \eta \sin \phi) = R(\pi)$, where ϕ and η are two arbitrary real numbers, we conclude that $\mathcal{U}_2 = e^{-iH_2t_2}$ should satisfy

$$\mathcal{U}_2 = e^{-i\pi K_0} e^{-i(K_1 \cos \phi + K_2 \sin \phi)\eta} \mathcal{U}_1^{-1}. \quad (20)$$

This SU(1,1) echo is analogous to the standard spin echo using SU(2) [17], and is applicable in a variety of bosonic systems. $\mathcal{U}_2\mathcal{U}_1$ corresponds to an arbitrary boost followed by a π rotation, $\mathcal{U}_2\mathcal{U}_1 = R(\pi)B(\eta \cos \phi, \eta \sin \phi)$. Equation (20) readily determines H_2 and t_2 . Since ϕ and η are arbitrary, for any H_1 , there is a family of H_2 , not just a single Hamiltonian, that could lead to the revival.

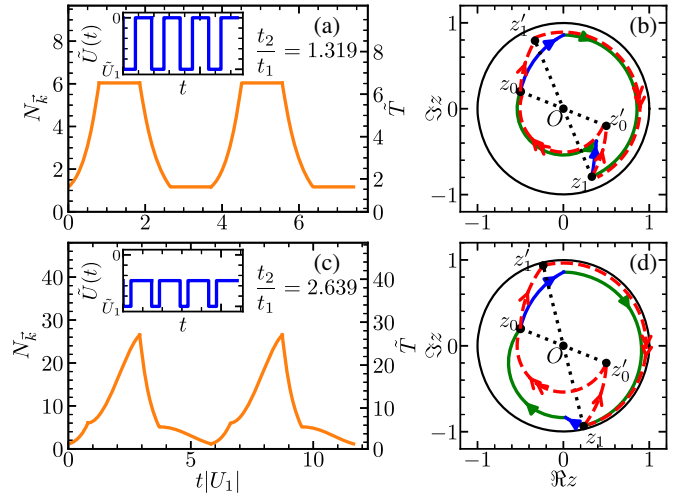


FIG. 3. SU(1,1) echoes. (a),(b) and (c),(d) The results of quenching the interaction from U_1 to 0 and $U_1/2e^{-i\pi/2}$, respectively, in the time interval from $t = t_1$ to t_2 . $t_1|U_1| = 0.8$, $E_{\vec{k}}/|U_1| = 1.3$. Insets show the modulation of interaction strength. Starting from any initial state z_0 , an appropriate t_2 guarantees that the system returns to the initial state after two periods of driving. Blue and green arrowed curves represent \mathcal{U}_1 and \mathcal{U}_2 , respectively. Red dashed curves with single and double arrows denote the boost, $B(\eta \cos \phi, \eta \sin \phi)$, and the rotation, $R(\pi)$, respectively, of $\mathcal{U}_1\mathcal{U}_2$.

Choosing $\eta = \eta_1$, $\phi = \phi_1 - \zeta_1$, we obtain $H_2 = u_0K_0$, and $t_2 = (\pi - 2\zeta_1)/u_0$. This means that quenching back to zero scattering length in Eq. (5) during the time interval from t_1 to t_2 reverses the quantum dynamics at $t = 2(t_1 + t_2)$, as shown in Fig. 3. Alternatively, if we quench the scattering length to a finite value, which amounts to a different choice of η and ϕ , the trajectory from $t = t_1$ to $t = t_2$ is no longer a concentric circle on the Poincaré disk. Nevertheless, an appropriate t_2 still leads to a quantum revival, as shown in Fig. 3. If we define $B(\eta \cos \phi, \eta \sin \phi)|z_0\rangle = |z'_1\rangle$, $B(\eta \cos \phi, \eta \sin \phi)|z_1\rangle = |z'_0\rangle$, we see that $z_0 = -z'_0$ and $z_1 = -z'_1$ are satisfied by both cases, providing us with a geometric interpretation of the quantum revival. We thus conclude, for any H_1 and t_1 , there is a family of H_2 to deliver $e^{-iH_2t_2} e^{-iH_1t_1} e^{-iH_2t_2} = e^{iH_1t_1}$. The SU(1,1) echo thus effectively creates a reversed evolution based on $-H_1$, an essential ingredient in studying OTOC [24–27].

We now consider interactions between excited particles. As the population of the resonant mode grows fastest when U is fixed, interactions at this mode become the dominant corrections. The Hamiltonian becomes $\tilde{H}_{\vec{k}} = H_{\vec{k}} + H'_{\vec{k}}$, where $H'_{\vec{k}} = U'(4c_k^\dagger c_{-\vec{k}} c_{-\vec{k}}^\dagger c_{-\vec{k}} + c_k^\dagger c_{-\vec{k}} c_{-\vec{k}}^\dagger c_k + c_{-\vec{k}}^\dagger c_k c_k^\dagger c_{-\vec{k}} - c_{-\vec{k}}^\dagger c_{-\vec{k}} c_{-\vec{k}}^\dagger c_k)$ can be rewritten as

$$H'_{\vec{k}} = 6U'(K_0 - 2/3)^2, \quad (21)$$

if the initial state is the two-mode vacuum. Without loss of generality, we have denoted the interactions between

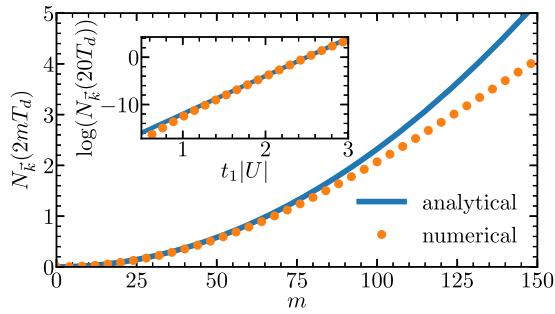


FIG. 4. The particle number at stroboscopic time mT_d . $U < 0$, $t_1|U| = 2.2$, $E_{\bar{k}}/|U| = 1$, and $U'/|U| = -5 \times 10^{-6}$. Inset shows the logarithm of $N_{\bar{k}}$ at $t = 20T_d$, confirming an exponential dependence of $t_1|U|$.

excited particles as U' . Here, $U' = \tilde{U}/2V$ but in other systems, U' might be independent of the unperturbed Hamiltonian. A finite U' breaks the $SU(1,1)$ symmetry, and an $SU(1,1)$ echo will not lead to a perfect revival of the initial state. The $SU(1,1)$ echo thus can be implemented as a unique tool to measure the interactions between excited particles, in the same spirit of using the spin echo to extract interactions between spins and other useful information. Using the $su(1,1)$ algebra, we obtain analytical results of the population at $t = 2mT_d$, $m \in \mathbb{N}$ [29],

$$N_{\bar{k}}(2mT_d) = \frac{27 \cosh(8\tilde{U}|\Psi_0|^2 t_1)}{16\tilde{U}^2|\Psi_0|^4} m^2 U'^2. \quad (22)$$

Confirmed by numerical calculations, Eq. (22) shows that $N_{\bar{k}}(2mT_d)$ vanishes when $U' = 0$. If $U' \neq 0$, $N_{\bar{k}}(2mT_d)$ increases quadratically as a function of m , as shown in Fig. 4. Thus, the imperfect revival unveils U' . In particular, $N_{\bar{k}}(2mT_d)$ depends on $\tilde{U}|\Psi_0|^2 t_1$ exponentially. Increasing t_1 could further improve the precision of the measurement. Alternatively, if U' is known, Eq. (22) allows experimentalists to measure $\tilde{U}|\Psi_0|^2 t_1$ with high precision due to the exponential dependence of $N_{\bar{k}}(2mT_d)$ on this parameter.

Whereas we have been focusing on quenching and periodically driving interactions in BECs, our results obtained by algebraic methods apply to any systems with the $SU(1,1)$ symmetry, including but not limited to the unitary fermions and 2D bosons and fermions with contact interaction [52–56]. For instance, $SU(1,1)$ echoes could be implemented to breathers of two-dimensional BECs, which was recently studied in an elegant experiment [57]. We hope that our work will stimulate more research efforts to unfold the intrinsic entanglement between dynamics, algebras, and geometries.

This work is supported by DOE DE-SC0019202, W. M. Keck Foundation, Purdue Research Foundation and a seed grant from Purdue Quantum Science and Engineering Institute.

*These authors contributed equally to this work.

†zhou753@purdue.edu

- [1] J. Maldacena, The large- N limit of superconformal field theories and supergravity, *Int. J. Theor. Phys.* **38**, 1113 (1999).
- [2] S. Sachdev, in *From Gravity to Thermal Gauge Theories: The AdS/CFT Correspondence* (Springer, Berlin Heidelberg, 2011), pp. 273–311.
- [3] S. Chapman, J. Eisert, L. Hackl, M. P. Heller, R. Jefferson, H. Marrochio, and R. C. Myers, Complexity and entanglement for thermofield double states, *SciPost Phys.* **6**, 034 (2019).
- [4] R. A. Jefferson and R. C. Myers, Circuit complexity in quantum field theory, *J. High Energy Phys.* **10** (2017) 107.
- [5] J. Maldacena and L. Susskind, Cool horizons for entangled black holes, *Fortschr. Phys.* **61**, 781 (2013).
- [6] J. Maldacena, Eternal black holes in anti-de Sitter, *J. High Energy Phys.* **04** (2003) 021.
- [7] F. Pastawski, B. Yoshida, D. Harlow, and J. Preskill, Holographic quantum error-correcting codes: Toy models for the bulk/boundary correspondence, *J. High Energy Phys.* **06** (2015) 149.
- [8] M. Nozaki, S. Ryu, and T. Takayanagi, Holographic geometry of entanglement renormalization in quantum field theories, *J. High Energy Phys.* **10** (2012) 193.
- [9] B. Swingle, Entanglement renormalization and holography, *Phys. Rev. D* **86**, 065007 (2012).
- [10] M. Miyaji, T. Numasawa, N. Shiba, T. Takayanagi, and K. Watanabe, Continuous Multiscale Entanglement Renormalization Ansatz as Holographic Surface-State Correspondence, *Phys. Rev. Lett.* **115**, 171602 (2015).
- [11] E. A. Donley, N. R. Claussen, S. L. Cornish, J. L. Roberts, E. A. Cornell, and C. E. Wieman, Dynamics of collapsing and exploding Bose-Einstein condensates, *Nature (London)* **412**, 295 (2001).
- [12] B. Wu and Q. Niu, Landau and dynamical instabilities of the superflow of Bose-Einstein condensates in optical lattices, *Phys. Rev. A* **64**, 061603(R) (2001).
- [13] J. H. V. Nguyen, D. Luo, and R. G. Hulet, Formation of matter-wave soliton trains by modulational instability, *Science* **356**, 422 (2017).
- [14] J. Hu, L. Feng, Z. Zhang, and C. Chin, Quantum simulation of Unruh radiation, *Nat. Phys.* **15**, 785 (2019).
- [15] C. C. Bradley, C. A. Sackett, J. J. Tollett, and R. G. Hulet, Evidence of Bose-Einstein Condensation in an Atomic Gas with Attractive Interactions, *Phys. Rev. Lett.* **75**, 1687 (1995).
- [16] J. Mun, P. Medley, G. K. Campbell, L. G. Marcassa, D. E. Pritchard, and W. Ketterle, Phase Diagram for a Bose-Einstein Condensate Moving in an Optical Lattice, *Phys. Rev. Lett.* **99**, 150604 (2007).
- [17] E. L. Hahn, Spin echoes, *Phys. Rev.* **80**, 580 (1950).
- [18] H. Bluhm, S. Foletti, I. Neder, M. Rudner, D. Mahalu, V. Umansky, and A. Yacoby, Dephasing time of GaAs electron-spin qubits coupled to a nuclear bath exceeding 200 μ s, *Nat. Phys.* **7**, 109 (2010).
- [19] E. L. Hahn and D. E. Maxwell, Spin echo measurements of nuclear spin coupling in molecules, *Phys. Rev.* **88**, 1070 (1952).

- [20] L. G. Rowan, E. L. Hahn, and W. B. Mims, Electron-spin-echo envelope modulation, *Phys. Rev.* **137**, A61 (1965).
- [21] P. F. Liao and S. R. Hartmann, Determination of Cr-Al hyperfine and electric quadrupole interaction parameters in ruby using spin-echo electron-nuclear double resonance, *Phys. Rev. B* **8**, 69 (1973).
- [22] X. Peng, H. Zhou, B.-B. Wei, J. Cui, J. Du, and R.-B. Liu, Experimental Observation of Lee-Yang Zeros, *Phys. Rev. Lett.* **114**, 010601 (2015).
- [23] A. W. Kinross, M. Fu, T. J. Munsie, H. A. Dabkowska, G. M. Luke, S. Sachdev, and T. Imai, Evolution of Quantum Fluctuations Near the Quantum Critical Point of the Transverse Field Ising Chain System CoNb_2O_6 , *Phys. Rev. X* **4**, 031008 (2014).
- [24] S. H. Shenker and D. Stanford, Black holes and the butterfly effect, *J. High Energy Phys.* **03** (2014) 067.
- [25] J. Maldacena, S. H. Shenker, and D. Stanford, A bound on chaos, *J. High Energy Phys.* **08** (2016) 106.
- [26] J. Li, R. Fan, H. Wang, B. Ye, B. Zeng, H. Zhai, X. Peng, and J. Du, Measuring Out-of-Time-Order Correlators on a Nuclear Magnetic Resonance Quantum Simulator, *Phys. Rev. X* **7**, 031011 (2017).
- [27] M. Gärttner, J. G. Bohnet, A. Safavi-Naini, M. L. Wall, J. J. Bollinger, and A. M. Rey, Measuring out-of-time-order correlations and multiple quantum spectra in a trapped-ion quantum magnet, *Nat. Phys.* **13**, 781 (2017).
- [28] C. Chin, R. Grimm, P. Julienne, and E. Tiesinga, Feshbach resonances in ultracold gases, *Rev. Mod. Phys.* **82**, 1225 (2010).
- [29] See Supplemental Material at <http://link.aps.org/supplemental/10.1103/PhysRevLett.125.253401>, which includes Refs. [30–39], for further discussions on the experimental realization, $\text{SU}(1,1)$ coherent states, controllable dynamics using periodic drivings, lengths of trajectories, and the increase of the particle number when the $\text{SU}(1,1)$ symmetry is broken.
- [30] R. Yamazaki, S. Taie, S. Sugawa, and Y. Takahashi, Submicron Spatial Modulation of an Interatomic Interaction in a Bose-Einstein Condensate, *Phys. Rev. Lett.* **105**, 050405 (2010).
- [31] T. L. Nicholson, S. Blatt, B. J. Bloom, J. R. Williams, J. W. Thomsen, J. Ye, and P. S. Julienne, Optical feshbach resonances: Field-dressed theory and comparison with experiments, *Phys. Rev. A* **92**, 022709 (2015).
- [32] R. R. Puri, *Mathematical Methods of Quantum Optics* (Springer, New York, 2001).
- [33] C. V. Parker, L.-C. Ha, and C. Chin, Direct observation of effective ferromagnetic domains of cold atoms in a shaken optical lattice, *Nat. Phys.* **9**, 769 (2013).
- [34] V. Galitski and I. B. Spielman, Spin-orbit coupling in quantum gases, *Nature (London)* **494**, 49 (2013).
- [35] C.-H. Li, C. Qu, R. J. Niffenegger, S.-J. Wang, M. He, D. B. Blasing, A. J. Olson, C. H. Greene, Y. Lyanda-Geller, Q. Zhou, C. Zhang, and Y. P. Chen, Spin current generation and relaxation in a quenched spin-orbit-coupled Bose-Einstein condensate, *Nat. Commun.* **10**, 375 (2019).
- [36] T.-L. Ho, Spinor Bose Condensates in Optical Traps, *Phys. Rev. Lett.* **81**, 742 (1998).
- [37] C. K. Law, H. Pu, and N. P. Bigelow, Quantum Spins Mixing in Spinor Bose-Einstein Condensates, *Phys. Rev. Lett.* **81**, 5257 (1998).
- [38] X.-Y. Luo, Y.-Q. Zou, L.-N. Wu, Q. Liu, M.-F. Han, M. K. Tey, and L. You, Deterministic entanglement generation from driving through quantum phase transitions, *Science* **355**, 620 (2017).
- [39] B. Yurke, S. L. McCall, and J. R. Klauder, $\text{SU}(2)$ and $\text{SU}(1,1)$ interferometers, *Phys. Rev. A* **33**, 4033 (1986).
- [40] C.-A. Chen and C.-L. Hung, Observation of modulational instability and Townes soliton formation in two-dimensional Bose gases, [arXiv:1907.12550](https://arxiv.org/abs/1907.12550).
- [41] M. Novaes, Some basics of $\text{su}(1, 1)$, *Rev. Bras. Ensino Fís.* **26**, 351 (2004).
- [42] Y.-Y. Chen, P. Zhang, W. Zheng, Z. Wu, and H. Zhai, Many-body echo, *Phys. Rev. A* **102**, 011301(R) (2020).
- [43] L.-Y. Chih and M. Holland, Driving quantum correlated atom-pairs from a Bose-Einstein condensate, *New J. Phys.* **22**, 033010 (2020).
- [44] R. Gilmore, *Lie Groups, Physics, and Geometry: An Introduction for Physicists, Engineers and Chemists* (Cambridge University Press, Cambridge, England, 2008).
- [45] Y. Cheng and Z.-Y. Shi, Many-body dynamics with time-dependent interaction, [arXiv:2004.12754](https://arxiv.org/abs/2004.12754).
- [46] M. O. Scully and M. S. Zubairy, *Quantum Optics* (Cambridge University Press, Cambridge, England, 1997).
- [47] C. C. Gerry, Correlated two-mode $\text{SU}(1, 1)$ coherent states: Nonclassical properties, *J. Opt. Soc. Am. B* **8**, 685 (1991).
- [48] S. W. Hawking, Black hole explosions?, *Nature (London)* **248**, 30 (1974).
- [49] W. G. Unruh, Notes on black-hole evaporation, *Phys. Rev. D* **14**, 870 (1976).
- [50] M. M. Wilde, *Quantum Information Theory* (Cambridge University Press, Cambridge, England, 2013).
- [51] S. Chapman, M. P. Heller, H. Marrochio, and F. Pastawski, Toward a Definition of Complexity for Quantum Field Theory States, *Phys. Rev. Lett.* **120**, 121602 (2018).
- [52] F. Werner and Y. Castin, Unitary gas in an isotropic harmonic trap: Symmetry properties and applications, *Phys. Rev. A* **74**, 053604 (2006).
- [53] S. Deng, Z.-Y. Shi, P. Diao, Q. Yu, H. Zhai, R. Qi, and H. Wu, Observation of the Efimovian expansion in scale-invariant fermi gases, *Science* **353**, 371 (2016).
- [54] D. T. Son, Vanishing Bulk Viscosities and Conformal Invariance of the Unitary Fermi Gas, *Phys. Rev. Lett.* **98**, 020604 (2007).
- [55] E. Elliott, J. A. Joseph, and J. E. Thomas, Observation of Conformal Symmetry Breaking and Scale Invariance in Expanding Fermi Gases, *Phys. Rev. Lett.* **112**, 040405 (2014).
- [56] C. C. Gerry, Berry's phase in the degenerate parametric amplifier, *Phys. Rev. A* **39**, 3204 (1989).
- [57] R. Saint-Jalm, P. C. M. Castilho, É. Le Cerf, B. Bakkali-Hassani, J.-L. Ville, S. Nascimbene, J. Beugnon, and J. Dalibard, Dynamical Symmetry and Breathers in a Two-Dimensional Bose Gas, *Phys. Rev. X* **9**, 021035 (2019).